

Schematic synthesis of cobalt-oxide (Co_3O_4) supported cobalt-sulfide (CoS) composite for oxygen evolution reaction

A. H. Samo^a, U. Aftab^b, D. X Cao^{a,*}, M. Ahmed^c, M. N. Lakhani^d, V. Kumar^e, A. Asif^f, A. Ali^g

^a*Key Laboratory of Superlight Material and Surface Technology, College of Materials Science and Chemical Engineering, Harbin Engineering University, PR China*

^b*Department of Metallurgy and Materials Engineering, Mehran University of Engineering and Technology, 76080, Jamshoro, Pakistan*

^c*Institute of Process Engineering, University of Chinese Academy of Sciences, PR China*

^d*School of Chemistry and Materials Science, University of Science and Technology of China, PR China*

^e*Department of Metallurgy and Materials Engineering, Dawood University of Engineering and Technology*

^f*College of Nuclear Science and Technology, Fundamental Science on Nuclear Safety and Simulation Technology Laboratory, Harbin Engineering University, PR, China*

^g*College of Underwater Acoustic Engineering, Harbin Engineering University, Harbin 150001, China*

Development of electrocatalysts has received great attention for storage and energy conversion technologies. Different electrocatalysts for oxygen evolution reaction (OER) have been produced and investigated but their role is not sufficient to mark of Ruthenium oxide (RuO_2). Therefore, it is global requirement to produce an efficient, lower cost and earth-abundant electrocatalyst for OER. Herein, cobalt oxide-cobalt sulfide ($\text{Co}_3\text{O}_4\text{-CoS}_2$) composite have been synthesized via hydrothermal chemical method with active performance OER. The desired overpotential is 280 mV to achieve current density of 20 mA cm^{-2} of as prepared composite with Tafel slope value of 74 mV dec⁻¹. As prepared $\text{Co}_3\text{O}_4\text{-CoS}_2$ composite has efficient stability of 30 hours for long term electrochemical performance.

(Received September 12, 2021; Accepted January 23, 2022)

Keywords: Hydrothermal method, Earth abundant, $\text{Co}_3\text{O}_4\text{-CoS}_2$ composite, Electrocatalyst, OER, Water splitting

1. Introduction

With increasing problems for global energy and environmental contaminations, utilization of electro catalysts favor to get renewable energy source [1, 2]. The water splitting method has been considered as an important base of modern chemical process, it has significance for oxygen evolution reaction (OER) and hydrogen evolution reaction (HER) [3, 4]. HER and OER have a dynamic role for production of hydrogen energy with less environment contamination [5, 6]. An efficient, low cost and electrochemically stable electrocatalyst for OER is still challenge for water

*Corresponding author: caodianxue@hrbeu.edu.cn

<https://doi.org/10.15251/DJNB.2022.171.109>

splitting. Previously, researchers have focused on substructure of efficient and earth abundant electrocatalysts [7, 8]. In previous studies, various precious metals have been reported such as Ir, and Ru base catalysts were utilized for OER applications as well. Due to their high cost, rare source and processing time make it still limited [9, 10]. OER is an essential reaction of electrochemistry that belong to storage system and power conversion, like fuel cells, water electrolyzes and metallic-air batteries [11, 12].

Some of the electrochemical characteristics of oxides have been used as cathodes and anodes in batteries or as electrocatalysts which have been reviewed briefly [13, 14]. In this regard, Jung et al. synthesized Co_3O_4 catalysts through transition of phase h-CoO into trigonal $\text{Co}(\text{OH})_2$ with better stability and outstanding electrochemical response compared with pristine Co_3O_4 [15]. Yu et al. prepared disordered cobalt oxide nanostructure induced by sulfur ($\text{S}-\text{CoO}_x$) that lead to more defect sites and enhanced low oxygen coordination, these features exhibit higher activity and efficient sustainability in alkaline electrolyte. Gao et al. reported improved catalytic activity by surface nitridation of Nickel-cobalt alloy ($\text{Ni}_2\text{-CoN}$), and found fast surface reconstruction that accelerates good active sites and stable for oxygen evolution [16]. Electrode potentials and stoichiometric reactions for the potential determination of various metal oxides have been discussed [17, 18].

Transition metal based electrocatalysts have been reported as an effective alternative of noble metal based electrocatalysts for OER such as; sNMs@NF [19], NiCo_2O [20], Mn-Fe oxide. Metal oxides are considered as encouraging electrode materials for conversion systems and energy storage including lithium-ion batteries (LIBs), hybrid super capacitors (HSCs), metal air batteries (MABs), sodium ion batteries (SIBs) and so on. Previous research report; sulfides of cobalt, like Co_9S_8 , CoS_2 , CoS have an essential activity of catalyst toward OER and HER both in alkaline medium with better chemical strength and electrical conductivity. There are various methods have been reported to prepare transitional metal nano composites such as; Liquid metal infiltration, Vapor techniques (PVD, CVD) and electrodeposition.

In this study, hydrothermal chemical method has been executed to synthesize $\text{Co}_3\text{O}_4\text{-CoS}_2$ composite for active OER performance. Pristine Co_3O_4 , pristine CoS and two composites were obtained by varying Co_3O_4 into CoS marked as Sample-1 and sample-2. An overpotential of 280 mV has been recorded to achieve 20 mA cm⁻² current density value with lower Tafel slope value of 74 mV dec⁻¹ by using Tafel equation. For morphology, crystallinity and chemical compound analysis SEM, XRD, TEM and FTIR were executed on pristine Co_3O_4 , CoS and as prepared composites (sample-1 and sample-2). EIS and CV were performed to obtain charge transfer resistance (R_{ct}), double layer capacitance (C_{dl}) and electrochemical active surface area (ECSA) measurement respectively. Above mentioned merits and various electrochemical results have proved that $\text{Co}_3\text{O}_4\text{-CoS}_2$ composite is an encouraging electrocatalyst for promising water splitting and energy conversion framework.

2. Experimental work

All the chemicals have been used in this experiment are of analytical grade and applied directly without any further purification. Thiourea ($\text{CH}_4\text{N}_2\text{S}$), cobalt chloride hexahydrate ($\text{Cl}_2\text{CoH}_{12}\text{O}_6$), potassium hydroxide (KOH), alumina slurry, and deionized water were purchased from Sigma-Aldrich Karachi.

$\text{Co}_3\text{O}_4\text{-CoS}_2$ composites were prepared by three phases. Initially, Co_3O_4 nano-structure was prepared by aqueous chemical growth process by taking 0.1M Cobalt chloride hexahydrate and 0.1M urea and placed for 5 h at 95°C into electric oven instrument by FOTILE 52L. The precipitates were collected and washed by deionized water for several times. Later on, calcination process was adopted on as received powder form of cobalt at 500°C in air to get its final product from hydroxide form. Finally, varying amount of 50 mg and 150 mg of Co_3O_4 were utilized for the decoration on CoS₂ by hydrothermal strategy at 200°C for 24 h. Thiourea 100 mM and cobalt chloride 40 mM concentration were used for CoS₂ solution and finally $\text{Co}_3\text{O}_4\text{-CoS}_2$ composites were obtained through filtration. Same strategy was applied for production of pristine CoS.

The morphological attributes were studied by executing low resolution scanning electron microscopy (Phillips, model CM 200 at 20 kV) at an advancing 15 kV voltage range. X-ray diffraction (Philips powder X-shaft diffractometer) was utilized to analyze crystallinity of pure Co_3O_4 , pure CoS and as prepared $\text{Co}_3\text{O}_4\text{-CoS}_2$ composite. Transmission electron microscopy instrument by FEI TECHNI G2 USA was used to determine the morphology of various nano materials in detail. FTIR instrument by PERKIN ELMER SPECTROPHOTOMETER was used for functional group study of various nanomaterials within wavenumber range of 400–4000 cm^{-1} .

The potentiostat machine by VERSA STAT4 was applied for different electrochemical tests. In three electrode mechanism Glassy carbon electrode (GCE) 3 mm diameter was used as working electrode, graphite bar as counter electrode and silver-silver chloride was used as reference electrode. At that point, 10 mg of every catalyst with 4 mL of deionized water was sonicated on ultrasonic bath to get proper homogeneous solution and 1 mL of 5% Nafion solution (as fastener) was used. 10 $\mu\text{-liter}$ of every Catalyst was covered on GCE and dried at room temperature, amount of impetus on GCE was about 0.30 mg cm^{-2} . Various electrochemical tests for OER activity were executed in 1M KOH solution. Initially linear sweep voltammetry was done by applying voltage ranges from 0 to 0.8V vs RHE. Cyclic voltammetry (CV) was carried with 0.1 to 0.25V at scan ranges from 30, 50, 70 and 90 mV s^{-1} . Electrochemical impedance spectroscopy (EIS) was done at voltage range of 5mV at frequency ranges from 100 kHz to 0.1 Hz. Stability practice was done at 20 and 40 mA cm^{-2} current densities through chronopotentiometry technique. Capacitance double layer (C_{dl}) values were calculated from CV curves of various nano materials. The results of EIS were illustrated by z-view software. Investigated potentials are described all over in manuscript in opposition to the reversible hydrogen electrode (RHE) through Nernst equation.

3. Results and discussion

Morphological study of different composites was analyzed via SEM as given in Fig. 1. Pristine CoS revealed round structure attributes containing various microns' level in Fig. 1(a). It reveals aggregation which is gathered by small flowery flakes. At contrasting, pure Co_3O_4 has been analyzed with nanoparticles as given in Fig. 1(b). While, Fig. 1(c) represents combined nanowire with round shape structures in sample-1 which shows availability of twice materials Co_3O_4 and CoS_2 in sample-1 ($\text{Co}_3\text{O}_4\text{-CoS}_2$ composite). Fig. 1(d) reveals structure of sample-2 containing mixture of round shape and nanowire with higher intensity due to addition of Co_3O_4 with more quantity. $\text{Co}_3\text{O}_4\text{-CoS}_2$ composite showed non-uniform morphologies as existence of two different attributes. Therefore, CoS_2 has a referable OER performance in sample-2 with various physical changes. At that point, the successful chemical growth of Co_3O_4 on CoS_2 can be observed through various SEM images.

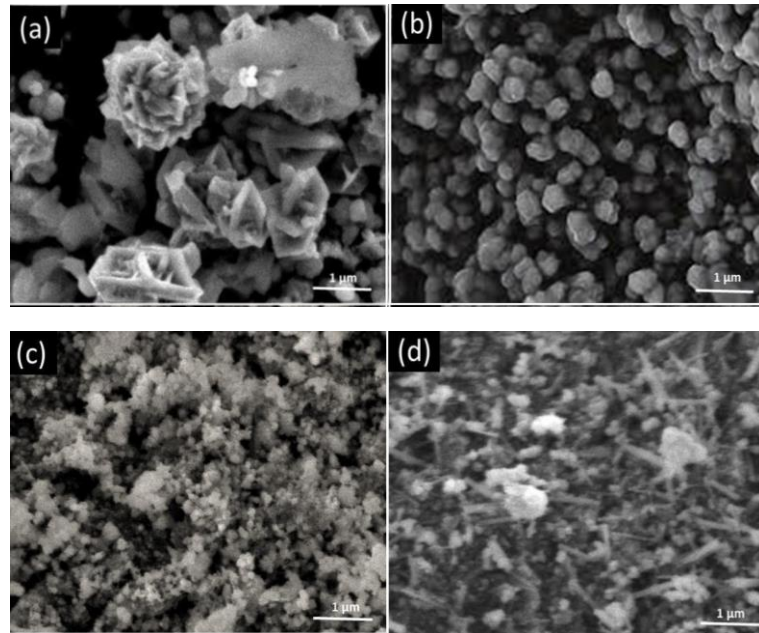


Fig 1. SEM images of various nano materials (a) CoS Pure, (b) Co_3O_4 Pure, (c) sample-1, (d) sample-2.

XRD technique has revealed the crystalline arrays of pristine CoS, Co_3O_4 and prepared composite as shown in Fig. 2. The pristine CoS diffraction patterns are intensive and resolved well, as it is confirmed by JCPDS card number: (01-075-0605) with hexagonal shape. XRD confirms that Pristine CoS has no other state of contaminations. The pristine Co_3O_4 shows well acute patterns which meet with the JCPDS card number: (01-080-1534) with cubic crystalline phase. Furthermore, it reveals that Co_3O_4 is pure, except of any other region of cobalt containing hydroxide and oxide phases as per given reference. XRD analysis was carried out for sample-2 and cubic phase is found within CoS_2 by JCPDS card number: (00-003-0772). We have obtained both CoS_2 and Co_3O_4 in our as prepared Co_3O_4 - CoS_2 composite material. XRD has assured that power of diffraction patterns of CoS_2 were decreased. Moreover, XRD study further described that Co_3O_4 - CoS_2 has no any other phase of impurities.

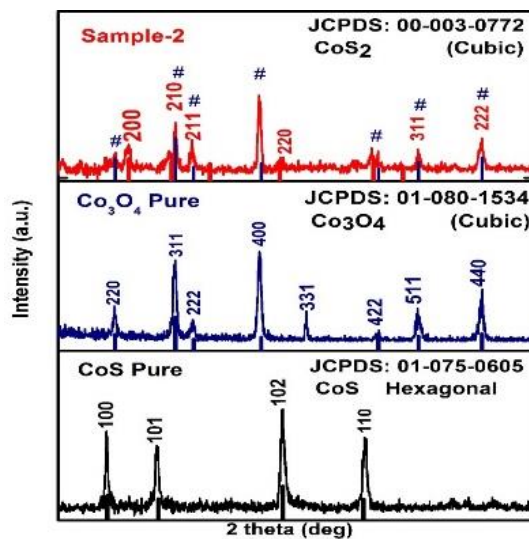


Fig. 2. Diffraction patterns of Pure CoS, Co_3O_4 and Sample-2.

Transmission electron microscopy (TEM) has been executed on various nanomaterials to analyze their surface morphology in deep way as depicted Fig. 3.

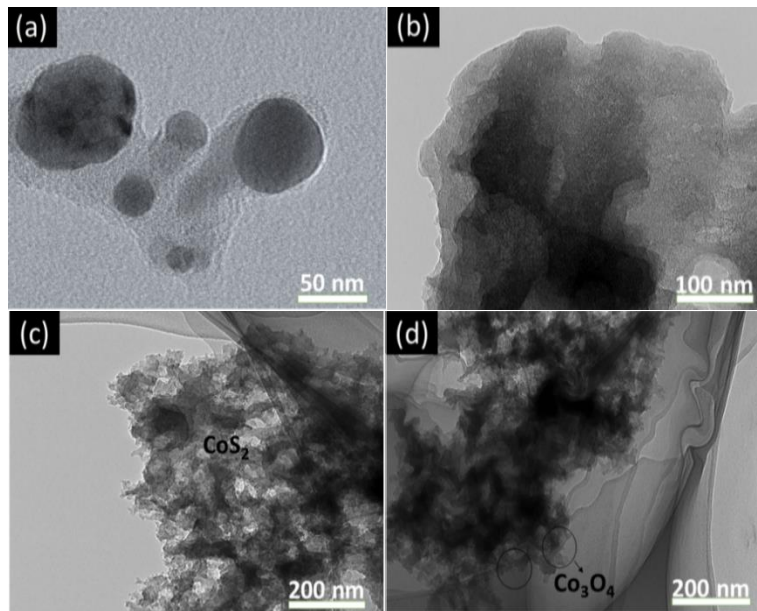


Fig. 3. TEM images of (a) Pristine Co_3O_4 , (b) Pristine CoS, (c) Sample-1 and (d) Sample-2.

Pristine Co_3O_4 has revealed its morphology as agglomerated nanoparticles with agreement to previous study as depicted in Fig. 3(a). The TEM image of CoS has shown hierarchical hollow nano-cages in detail as shown in Fig. 3(b). Uniform CoS layers are consisting of monodispersed layered structure. These outer nanoparticles of CoS have rough surfaces type morphology. As prepared composites sample-1 and sample-2 have similar structural characteristics with changes in intensity of Co_3O_4 within CoS_2 as given in Fig. 3(c) and (d) respectively. There is existence of Co_3O_4 nanoparticles with varying quantity which is clearly observed at different boundaries in core of CoS_2 and outer bright translucent shell within sample-1 and sample-2. The successful synthesis of Co_3O_4 - CoS_2 composite has been observed from various TEM images for synergistic electrochemical performance for OER activity.

The FTIR analysis was applied for pristine CoS, Co_3O_4 and as prepared composite electrocatalyst. IR spectra of Co_3O_4 nanocomposite is shown in supplementary information as Fig. (S1). Broad band at 3440 cm^{-1} is because of stretching vibration mode of O-H group. Band around 848 cm^{-1} is due to peaks of CO_3^{2-} anions. Two peaks at 574 and 670 cm^{-1} have correspondence to Co-O stretching vibration mode. Whereas, the relevant band at 1110 cm^{-1} along with spectrum of CoS relevant to the N-H bending vibration. To evaluate structure of sample-2 via FTIR is also mentioned in given corresponding figure, another peak at 570 cm^{-1} stretching vibrations of Co atoms have been observed on the surface of cobalt sulfide as relevant small peak.

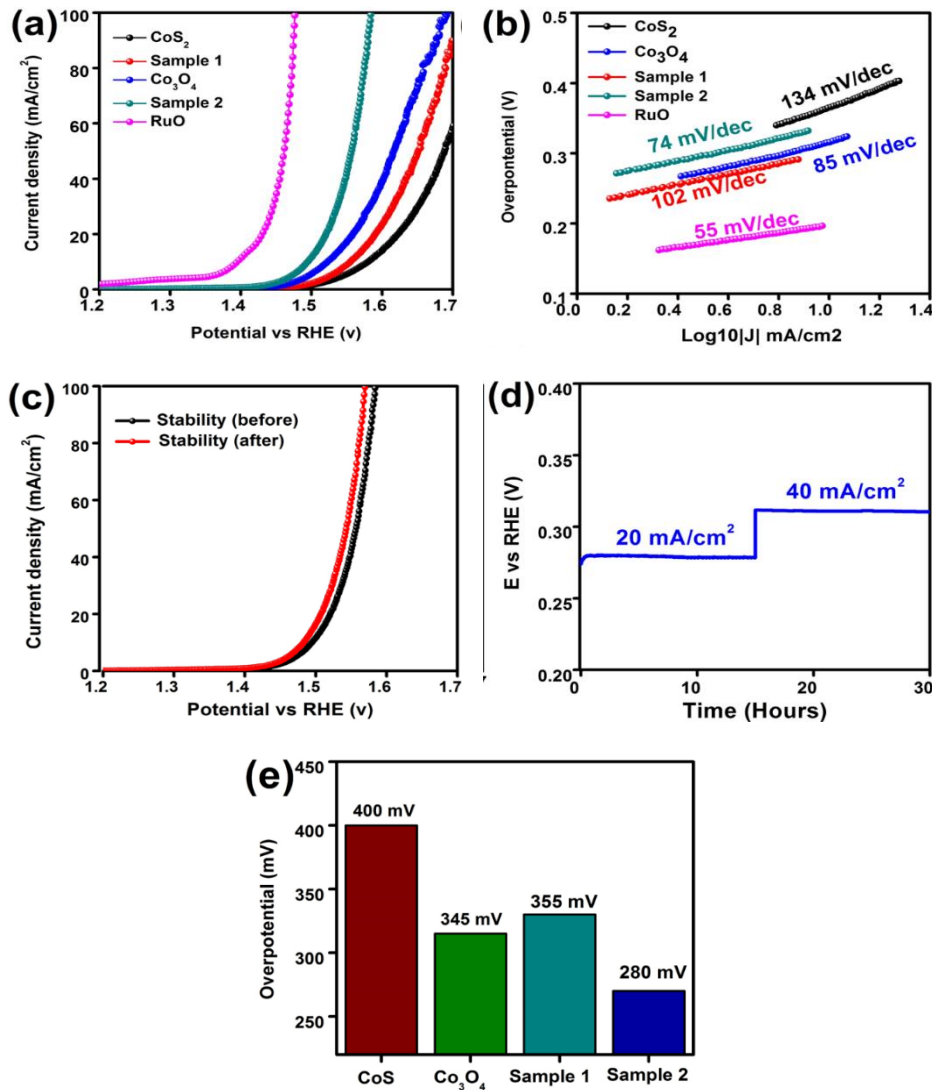


Fig. 4. (a) LSV curves of pure CoS , pure Co_3O_4 , sample-1 and sample-2, (b) Tafel plots, (c) Durability practice, (d) Chronopotentiometry at 20 and 40 mA cm^{-2} for 30 h, (e) Histogram for overpotential values.

Electrochemical tests of different electrocatalysts were studied in 1M KOH using three-electrode system for OER activity. LSV polarization strategy for CoS , Co_3O_4 and its composites Sample-1 and Sample-2 are shown in Fig. 4. It is highlighted that pure CoS and Co_3O_4 have not good OER activity, by addition of Co_3O_4 for good appearance of CoS_2 has dramatically increase in OER kinetics. Supplementary addition of Co_3O_4 for deposition has also shown great role in conductivity and capacitance as well. Sample-2 has more activity because of fast charge transport given through Co_3O_4 single dimensional nanowires, along with active sites from CoS_2 and good stoichiometry of Co presence has revealed essential OER kinetics. As prepared composite of Co_3O_4 - CoS_2 marked as sample-2 has over all good OER response more than both of given pristine forms which is shown in Fig. 4(a).

The overpotential value of 280 mV is required to reach at current density of 20 mA cm^{-2} for sample-2, which is better than sample-1 that has overpotential value of 355 mV. From LSV curves, Co_3O_4 - CoS_2 composite material along with specific amount of Co_3O_4 can enhance OER performance of CoS_2 . Meanwhile it could be an excellent alternative of noble metal containing electrocatalyst for OER. Tafel plot is essential factor for OER activity of electrocatalyst as rate-determination step ³⁷, as shown in Fig. 4(b). It assured that pure CoS_2 and Co_3O_4 have poor electrochemical response. Sample-2 has Tafel slope value of 74 mV dec⁻¹ which is lowest toward cobalt based electrocatalyst for OER and nearer to Tafel slope value of RuO as 55 mV dec⁻¹.

Sample-1 has higher Tafel slope of 102 mV dec⁻¹. Therefore, on the basis Tafel slope analysis we can report that OER activity of Sample-2 is closer to noble metal based electrocatalyst. As depicted in Fig. 4(c) durability of sample-2 was analyzed before and after stability test. The chronopotentiometry technique was applied at 20 and 40 mA cm⁻² current densities for stability, without any loss of potential was observed as clearly shown in Fig. 4(d). While corresponding overpotential value of every electrocatalyst is described in histogram as given in Fig. 4(e).

Basically, OER mechanism contains four electron transfer system which could be described over the surface of desired metal oxide in alkaline environment as given four steps below;



Above given four steps mechanism has its theoretical Tafel values as per steps 1 to 4 are 120, 60, 40 and 15 mV dec⁻²³⁸. However, in this work the rate determining step for Co₃O₄-CoS₂ electrocatalyst is step 3 as per obtained Tafel slope value from given relation.

$$\eta = a + b \log(j) \quad (5)$$

where η defines overpotential value, j defines current density and b defines Tafel slope respectively³⁹.

To make more strength of polarization and Tafel curves, OER kinetics of electrocatalyst was measured through electrochemical impedance spectroscopy (EIS) in 1M KOH solution. The value of charge transfer rate has been defined via diameter of semicircle arc and analyzed R_{ct} value for sample-1 is 280 Ω, that is higher than the composite of sample-2 which has value of 85 Ω respectively. These both values are several times less than pristine CoS and Co₃O₄ as obtained 1250 and 905 Ω. It has been confirmed that faster charge transport is related to Sample-2 composite is due to addition of Co₃O₄. For similar electrochemical impedance spectroscopy results, bode plots were obtained as appeared in Fig. 5 (a) and (b) which support more to Nyquist plots. Nyquist plots of various composites are given in Fig. 5 (c). However, Cyclic voltammetry (CV) was applied at various scan rates for calculation of ECSA and C_{dl} as given in supplementary information which is depicted in supplementary file as Fig. (S2). CV was carried out at scan rate of 30, 50, 70 and 90 mV sec⁻¹ for pristine CoS, Co₃O₄ and composites sample-1 and sample-2 along with pristine GCE as its supportive information. The corresponding C_{dl} values are calculated as 4.0 μF cm⁻² for pristine Co₃O₄, 5.3 μF cm⁻² for pristine CoS, 8.2 μF cm⁻² for Sample-1 and highest one for sample-2 is 20 μF cm⁻². The obtained ECSA values of various composites were calculated from C_{dl} values through given expression.

$$ECSA = C_{dl} / C_s \quad (6)$$

where, C_{dl} represent double layer capacitance value and C_s specific capacitance (i-e., C_s=0.04 μF cm⁻²) for KOH environment. Through this expression, analyzed values of ECSA for various electrocatalysts are as 100, 132.5, 205 and 500 cm² for pristine Co₃O₄, CoS, sample-1 and sample-2 which are mentioned below in Table 1. The enhanced value of ECSA for sample-2 put impact for addition of Co₃O₄ as its vital role toward effective OER activity.

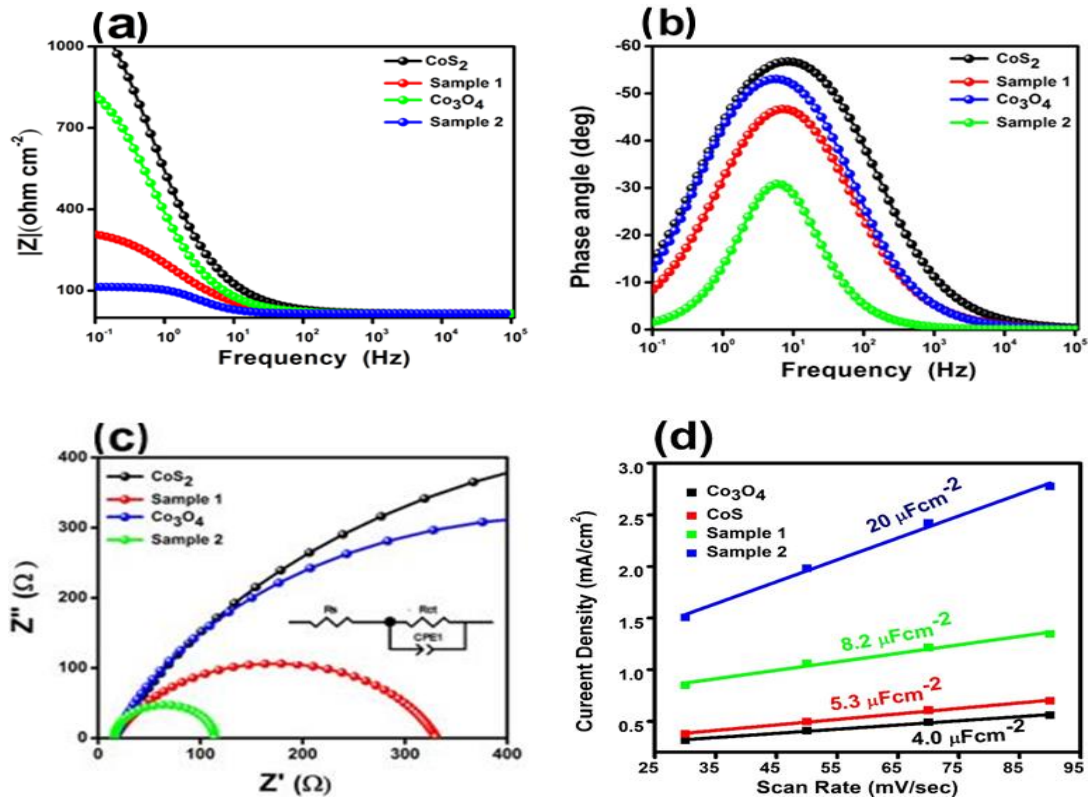


Fig. 5. EIS of pure CoS, pure Co₃O₄, Sample-1, Sample-2 by amplitude of 5 mV with frequency ranges from 100 KHz to 0.1 Hz, with settled potential of OER (a, b) bode plots (c) Nyquist plots (d) Corresponding C_{dl} values by linear fitting at different scan rates from CV curves for of Co₃O₄, CoS, sample-1 and sample-2.

Table 1. Unique Features of reported OER electrocatalysts.

Catalyst	Tafel Slope	Charge Transfer Resistance	Double Layer Capacitance	Electrochemical Active Surface Area
	<u>B</u>	<u>R_{ct}</u>	<u>C_{dl}</u>	<u>ECSA</u>
	<u>mV dec⁻²</u>	<u>Ω</u>	<u>(μF cm⁻²)</u>	<u>cm²</u>
Co ₃ O ₄ Pristine	85	905	4.0	100
CoS Pristine	134	1250	5.3	132.5
Sample-1	102	280	8.2	205
Sample-2	74	85	20	500

4. Conclusion

In conclusion, different substances are integrated containing pure CoS, Co₃O₄ and as prepared composites with varying ratio of Co₃O₄ via hydrothermal chemical strategies and analyzed for OER activity. This Co₃O₄-CoS₂ based electrocatalyst has indicated an incredible electrochemical performance for OER. Sample-2 displayed excellent electrical conductivity with lower overpotential value of 280 mV as compared to pristine Co₃O₄, pristine CoS and Sample-1 at 20 mA cm⁻² current density in alkaline environment. Moreover, durability of 30h was observed for Co₃O₄-CoS₂ (sample-2). The lower Tafel slope value of 74 mV dec⁻¹ with lower charge transfer resistance value 85 Ω for sample-2 proved it more active for oxygen evolution. As calculated larger ECSA value of 500 cm² has correspondence to more capacitive behavior of Co₃O₄-CoS₂ composite as well. SEM, XRD, TEM and FTIR have analyzed the morphology, crystallinity and

functional groups of various electrocatalysts. In this way, $\text{Co}_3\text{O}_4\text{-CoS}_2$ based electrocatalyst is well considered for a wide scope of energy conversion and electrochemical water splitting applications.

Acknowledgements

All the authors are thankful to financial support of the National Natural Science Foundation of China (NSFC 51402065 and 51603053), the Natural Science Foundation of Heilongjiang province (LH2019E025), National Defense Industrial Technology Development program (JCKY2016604C006), and the National Key Research and Development program of China (2016YFE0202700).

References

- [1] L. Yaqoob et al., Journal of Alloys and Compounds **850**, 156583 (2021).
- [2] A. Naderi et al., Applied Surface Science **542**, 148681 (2021).
- [3] J. Yang, Y. Fan, P.-F. Liu, Applied Surface Science **540**, 148245 (2021).
- [4] L. Yaqoob et al., Renewable Energy **156**, 1040 (2020).
- [5] J. Ding et al., International Journal of Hydrogen Energy **44**, 2832 (2019).
- [6] D. Chen et al., Applied Catalysis B: Environmental **268**, 118729 (2020).
- [7] R. A. E. Acedera, G. Gupta, M. Mamlouk, M. D. L. Balela, Journal of Alloys and Compounds **836**, 154919 (2020).
- [8] P. T. Babar et al., Journal of Industrial and Engineering Chemistry **60**, 493 (2018).
- [9] A. Wu et al., Nano Energy **44**, 353 (2018).
- [10] S. K. Meher, G. R. Rao, The Journal of Physical Chemistry C **115**, 15646 (2011).
- [11] J.-H. Kim et al., Applied Catalysis B: Environmental **225**, 1 (2018).
- [12] W. H. Lee et al., Applied Catalysis B: Environmental **269**, 118820 (2020).
- [13] K. Liu et al., Journal of Alloys and Compounds **725**, 260 (2017).
- [14] A. L. Bhatti et al., RSC Advances **10**, 12962 (2020).
- [15] H. Jung et al., Chemical Engineering Journal, 127958 (2020).
- [16] X. Gao et al., Applied Catalysis B: Environmental **270**, 118889 (2020).
- [17] W. Liu et al., Journal of Energy Chemistry, (2020).
- [18] B. M. Hunter, H. B. Gray, A. M. Müller, Chemical Reviews **116**, 14120 (2016).
- [19] L. Pei et al., Electrochimica Acta, 137651 (2020).
- [20] C. Bocca, A. Barbucci, M. Delucchi, G. Cerisola, International Journal of Hydrogen Energy **24**, 21 (1999).

Supplementary Material

Schematic synthesis of cobalt-oxide (Co_3O_4) supported cobalt-sulfide (CoS) composite for oxygen evolution reaction

A. H. Samo^a, U. Aftab^b, D. X. Cao^{a*}, M. Ahmed^c, M. N. Lakhani^d, V. Kumar^e, A. Asif^f, A. Ali^g

^a*Key Laboratory of Superlight Material and Surface Technology, College of Materials Science and Chemical Engineering, Harbin Engineering University, PR China*

^b*Department of Metallurgy and Materials Engineering, Mehran University of Engineering and Technology, 76080, Jamshoro, Pakistan*

^c*Institute of Process Engineering, University of Chinese Academy of Sciences, PR China*

^d*School of Chemistry and Materials Science, University of Science and Technology of China, PR China*

^e*Department of Metallurgy and Materials Engineering, Dawood University of Engineering and Technology*

^f*College of Nuclear Science and Technology, Fundamental Science on Nuclear Safety and Simulation Technology Laboratory, Harbin Engineering University, PR, China*

^g*College of Underwater Acoustic Engineering, Harbin Engineering University, Harbin 150001, China*

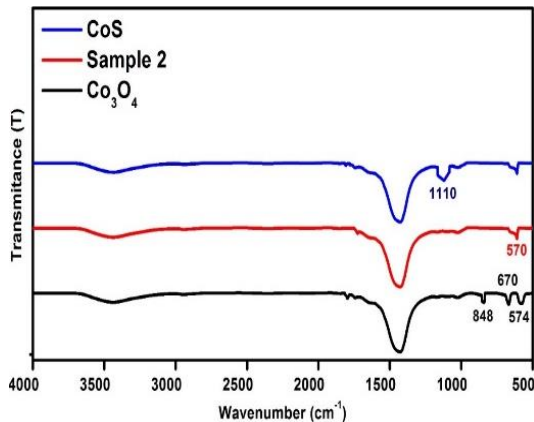
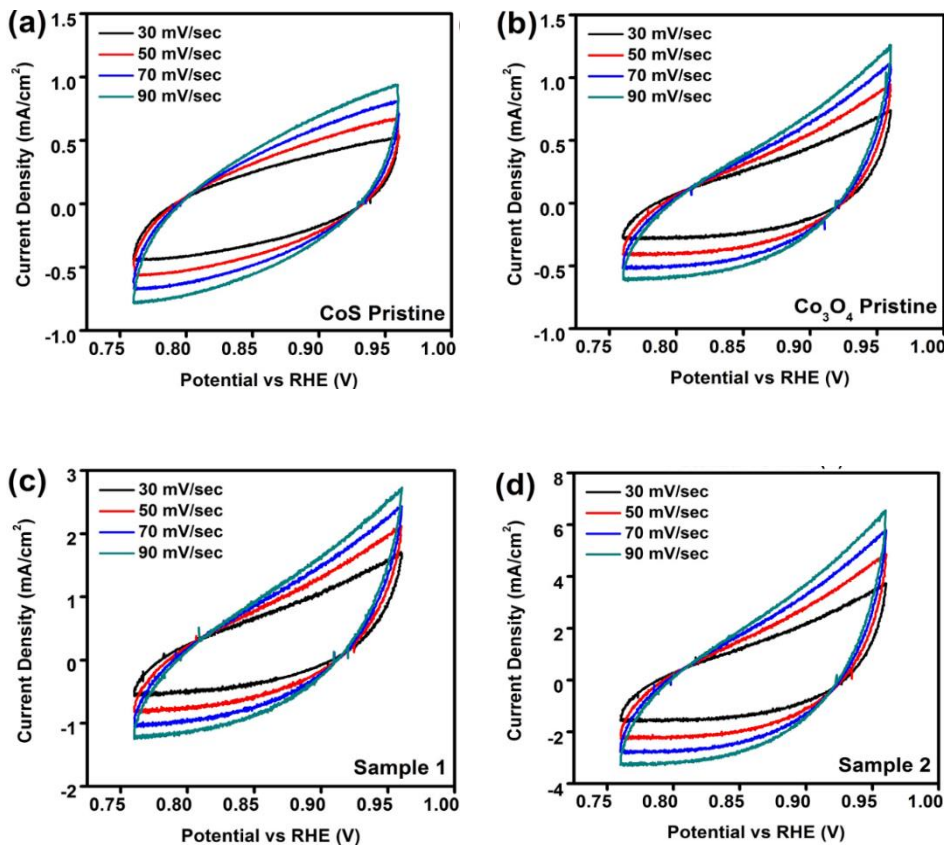


Fig. S1. FTIR spectra of pristine Co_3O_4 , pristine CoS and prepared sample-2.

Table S1. Comparative study of recent reported electrocatalysts and current work.

<u>Electrocatalyst</u>	<u>Electrolyte</u>	<u>Current density</u>	<u>Overpotential</u>	<u>Tafel slope</u>	<u>Reference</u>
Sample-2 (Co_3O_4 - CoS_2)	1M KOH	20 mA/cm ²	280 mV	74 mV/dec	This work
Spinel Co_3O_4	1M KOH	10 mA/cm ²	296 mV	92 mV/dec	[1]
Ni-Co-F	1M KOH	10 mA/cm ²	326 mV	77 mV/dec	[2]
Mesoporous Co_3O_4 nanosheet	1M KOH	10 mA/cm ²	290 mV	86 mV/dec	[3]
Ru/Ni- Co_3O_4	1M KOH	10 mA/cm ²	290 mV	70 mV/dec	[4]
$\text{Co}_3\text{S}_4/\text{Ni}$	1M KOH	10 mA/cm ²	283 mV	65 mV/dec	[5]
CoMn_2O_4 -MSs	0.1M KOH	10 mA/cm ²	300 mV	72 mV/dec	[6]
CoS_2 -TF	1M KOH	10 mA/cm ²	295 mV	57 mV/dec	[7]
MOF-driven CoS_2	1M KOH	10 mA/cm ²	298 mV	98 mV/dec	[8]

Fig. S2. CV curves with varying scan rates of 30, 50, 70 and 90 mV/sec in 1M KOH (a) pure CoS, (b) pure Co_3O_4 , (c) sample-1, (d) Sample-2.

References

- [1] B. Paul, P. Bhanja, S. Sharma, Y. Yamauchi, Z. A. Alothman, Z.-L. Wang et al., Journal of Colloid and Interface Science 582, 322 (2021); <https://doi.org/10.1016/j.jcis.2020.08.029>
- [2] Y. Xue, Y. Wang, H. Liu, X. Yu, H. Xue, L. Feng, Chemical communications 54, 6204 (2018); <https://doi.org/10.1039/C8CC03223H>
- [3] T. Xie, J. Min, J. Liu, J. Chen, D. Fu, R. Zhang et al., Journal of Alloys and Compounds 754, 72 (2018); <https://doi.org/10.1016/j.jallcom.2018.04.207>

- [4] B. Guo, R. Ma, Z. Li, J. Luo, M. Yang, J. Wang, Materials Chemistry Frontiers 4, 1390 (2020);
<https://doi.org/10.1039/D0QM00079E>
- [5] S. Tang, X. Wang, Y. Zhang, M. Courté, H. J. Fan, D. Fichou, Nanoscale 11, 2202 (2019);
<https://doi.org/10.1039/C8NR07787H>
- [6] A. Bahadur, W. Hussain, S. Iqbal, F. Ullah, M. Shoaib, G. Liu et al., Journal of Materials Chemistry A 9, 12255 (2021); <https://doi.org/10.1039/D0TA09430G>
- [7] S. B. Kale, A. C. Lokhande, R. B. Pujari, C. D. Lokhande, J Colloid Interface Sci. 532, 491 (2018); <https://doi.org/10.1016/j.jcis.2018.08.012>
- [8] I. K. Ahn, W. Joo, J. H. Lee, H. G. Kim, S. Y. Lee, Y. Jung et al., Scientific reports 9, 19539 (2019); <https://doi.org/10.1038/s41598-019-56084-9>